Available online at www.CivileJournal.org

Civil Engineering Journal

(E-ISSN: 2476-3055; ISSN: 2676-6957)

Vol. 12, No. 05, May, 2026

Residential Building Resilience Model Against Seismic Disaster with Fuzzy Logic–Fragility Analysis Approach

Setiono [1], Senot Sangadji [1*], Stefanus A. Kristiawan [1], Nur Miladan [2]

[1] *Department of Civil Engineering, Sebelas Maret University, Surakarta 57126, Indonesia.*

[2] *Urban and Regional Planning Department, Sebelas Maret University, Surakarta 57126, Indonesia.*

Received 12 December 2025; Revised 11 April 2026; Accepted 17 April 2026; Published 01 May 2026

Abstract

Residential buildings are part of the urban physical infrastructure most affected by a seismic disaster. The resilience (R) of residential buildings should be evaluated for disaster mitigation before, during, and after disasters to minimize potential damage. This study proposed an R evaluation model for residential buildings that combined a fragility analysis and a fuzzy logic approach. The developed model combined the functionality (q) and recovery time (t) to obtain the R index. A fragility analysis was used to calculate the q of residential buildings, where the t was normalized to the longest possible t (0–1) for input into the fuzzy inference process, which depended on government decisions and other factors, including the available budget and other conditions. Resilience (R) was computed using a fuzzy logic (FL) approach with the Tsukamoto inference system. The research resulted in a model for evaluating the R of residential buildings for seismic disasters. The value of the research lies in the conversion of probabilistic damage decisions into fuzzy representations of post-earthquake q and t, so that both variables can be coupled within a single decision-focused model. The model was applied to simulate the R of residential buildings in Surakarta City during an earthquake. One- and two-story buildings accounted for more than 98% of the residential building data. The R for residential buildings under the applied scenario for a spectral acceleration (Sa) of 0.16 g was quantified at 52.47%, indicating a condition of moderate resilience. The developed model can help the government to evaluate the R of residential buildings and can be adjusted for other components of urban infrastructure, such as transportation, electricity, and telecommunication networks.

Keywords: Earthquake; Fragility Analysis; Fuzzy Logic; Resilience; Residential Buildings; Tsukamoto Inference.

1. Introduction

Indonesia faces significant seismic hazards due to its position on the Circum-Pacific Belt [1], which significantly threatens its infrastructure, including constructed buildings. Several earthquakes have occurred across various regions of Indonesia, resulting in numerous fatalities [2]. Seismic risk can manifest as the risk of death [3, 4] and the risk of damage to essential buildings, such as residential buildings, schools, hospitals, and others. Most earthquake-related building destruction in Indonesia involves residential buildings, such as those in Aceh [5], Yogyakarta [6], Lombok [7], Palu [8], West Java [9], and East Java [10]. Many residential buildings in Indonesia are built by their owners, and thus, their quality varies according to the economic capability of the owners to provide building materials and labor. Sometimes, due to the lack of construction standards, residential buildings are often called non-engineered buildings [11].

* Corresponding author: s.sangadji@staff.uns.ac.id

https://doi.org/10.28991/CEJ-2026-012-05-015

In contrast to risk, resilience (*R*) refers to the capacity of a system to absorb, adapt, and recover from stress, disturbances, or disasters [12]. In a broader sense, the *R* of a region or city encompasses aspects of the population, physical infrastructure, governance, economy, social life, and environment [13, 14]. Resilience (*R*) can also be measured in greater detail, for example, through the physical infrastructure dimension. It can also support decision-making in disaster risk mitigation efforts before, during, and after a disaster strikes a region, helping to minimize losses.

Figure 1 illustrates the hierarchy of city-wide *R*, encompassing all dimensions of a real-world city, including its physical infrastructure. It consists of components such as building construction, transportation, clean water, waste, electricity, telecommunication, wastewater, and drainage networks, down to the city's physical infrastructure dimension, *R*, and its components. Residential buildings are part of the building construction component and are vital as places where people live.

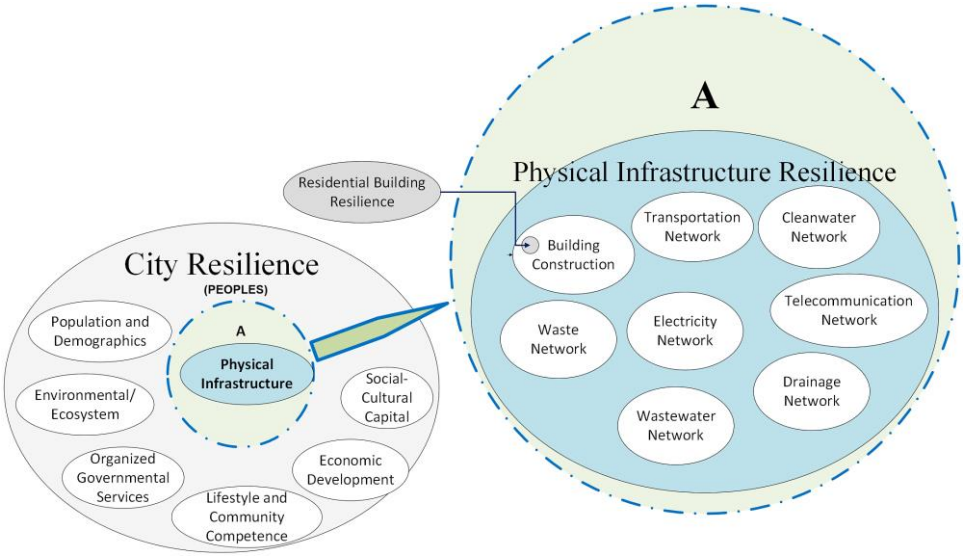

Figure 1. Residential buildings in the city's resilience scope, adapted from [15]

Generally, the *R* of a system is based on two variables, namely, functionality (*q*), and recovery time (*t*) (Figure 2). Functionality (*q*) is the level of service performance of any dimension or component of a system, where *t0* represents the time before a disaster, *t1* represents the time after a disaster, and *t2* represents the time after recovery has been fully undertaken. When an earthquake occurs, the system's *q* decreases, and over time, with recovery efforts, it returns to its desired or original level. Normally, *q* is considered to be 100% (full *q*), while *t* depends on various factors, including government policy, and can vary from one system to another. Therefore, it needs to be normalised to a range of 0–100%. The uncertainty relationship between *q* and *t* can be bridged by using a fuzzy logic (FL) approach [16].

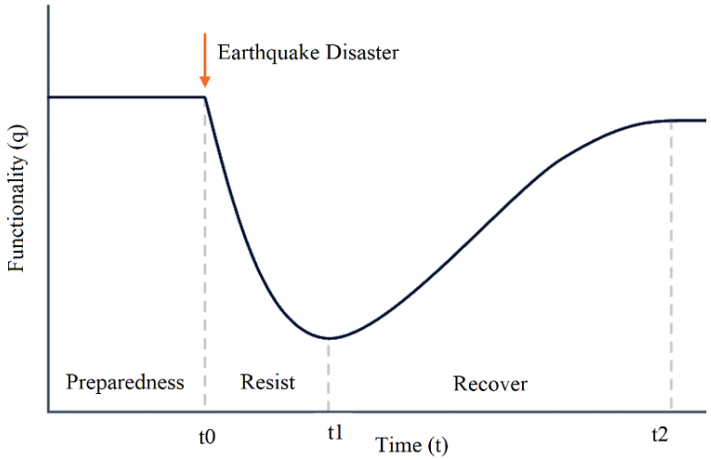

Figure 2. Schematic of seismic resilience of a system

Several studies examined seismic R in buildings and residential buildings. Tasmen et al. built a framework with Dynamic Bayesian Networks (DBN) to evaluate urban housing infrastructures. It was utilized to measure seismic *R* in study areas in Japan [17]. Altunışık et al. developed empirical fragility curves for reinforced concrete residential buildings in Türkiye, categorizing them by age and height. They found that the age of a building is related to its

vulnerability [18]. Zhao et al. developed an innovative dynamic repair scheduling approach that effectively incorporates two essential construction-related parameters, namely, the prefabrication ratio and the types of prefabricated components. By integrating these factors, the method enables more precise estimates of the *t* trajectories and downtime, ultimately enhancing the efficiency of construction projects [19]. Wang et al. proposed a new methodology for predicting the functional *t* of a damaged area. This method considers performance-based repair objectives, different damage states (*ds*), and the size of the affected building area. It enhances the standard approach of categorizing damaged buildings into repairable and reconstructive categories by incorporating the *ds* parameter of the building [20].

Naiel et al. developed fragility curves for mid-rise reinforced concrete residential buildings, demonstrating how reinforced concrete design codes influence vulnerability and *R* [21]. Chen et al. studied how corrosion and deterioration affect fragility curves and reduce *R* indices over the service life of reinforced concrete buildings, showing the effects of time on vulnerability [22]. Formisano and Longobardi evaluated the performance of the existing compound through a macro element modeling approach and arranged a lightweight retrofitting solution designed to improve the building's seismic response and promote its box-like structural behavior, developed fragility curves for masonry compounds, and used lightweight exoskeleton retrofits [23]. Dahal et al. developed a comprehensive framework for assessing the regional seismic risk and *R* of large building inventories, enabling stakeholders to identify vulnerable buildings and prioritize interventions at the community scale [24]. Jia et al. developed a life-cycle seismic *R* and sustainability assessment method for reinforced concrete buildings that combines deterioration effects with stochastic earthquake processes, aimed at quantifying *R* over a building's service life and supporting long-term planning [25].

Previous research evaluated seismic *R* using fragility curves, Bayesian models, and expressions for *t*. These techniques estimate the *ds*, or *t*, appropriately; however, they decouple *q* from *t*. They also require a sharp *ds* and exact inputs, which are not indicative of post-earthquake uncertainty in residential buildings. The probability of damage (*P*) seldom translates to a single *R* index in fragility-based studies. Recovery-related studies predict functional trajectories but do not account for frailty-related uncertainty. No research has been explicitly conducted that combines a fragility analysis with the FL methodology to relate building functions and *t* within a single *R* framework. This integration enables probabilistic damage outcomes and post-disaster recovery considerations to be unified within a single, interpretable resilience index that directly supports decision-making in seismic risk mitigation. The model developed in this study is a combination of a fragility analysis [26, 27] and FL with the Tsukamoto inference [28]. The developed model is expected to facilitate the assessment of the *R* of residential buildings, enabling *R* to be estimated in the event of an earthquake. The FL and the fragility analysis offer a novel approach for assessing the seismic *R* of residential buildings by explicitly accounting for uncertainty in the *ds*, *q*, and *t*. Ultimately, the evaluation model developed will be applied to residential buildings in Surakarta City.

This paper is organized as follows. Section 2 outlines the research procedure, including the fragility analysis, calculation of *q*, determination of *t*, and the fuzzy inference system. Section 3 presents the results and discussion, covering the membership function model, the calculation of the *q* of residential buildings, and the assessment of the *R* of one- and two-story residential buildings. The final section, Section 4, concludes the paper.

2. Research Method

Figure 3 shows the process undertaken in this research to develop an evaluation model for the *R* of residential buildings. The first step was the literature review of the fragility analysis method and the FL algorithm. Data were collected from a survey of residential buildings in an urban area to obtain their properties. A fragility analysis using Seismostruct was employed to determine the *q* for the surveyed residential building sample. Accordingly, the FL approach, utilizing the Tsukamoto fuzzy inference system, was employed to calculate the *R*.

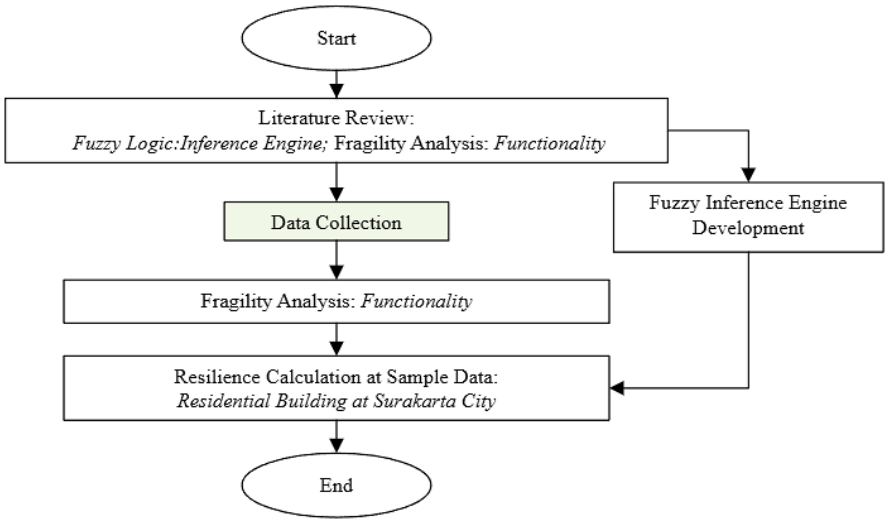

Figure 3. Resilience Evaluation Model Development Process

The *R* calculation model relied on two independent variables, namely, *q* and *t*, and one dependent variable, namely, *R*. The relationship between the *q* and *t* variables was determined using an FL model adapted from Kammouh et al. [29]. This research also tried to refine the membership functions for *q* and the target *R* to obtain more accurate results. The flowchart in Figure 4 explains the sequence of processes that occurred in the *R* calculation model, with input data in the form of *q* and *t* ranging from 0–100% for both. Next, both inputs were transformed into fuzzy numbers according to their membership functions by the *fuzzification* process. Both the fuzzified *q* and *t* were processed based on a rule base implemented in the inference engine, resulting in the fuzzy *R*, which was then de-fuzzified to obtain the crisp *R*.

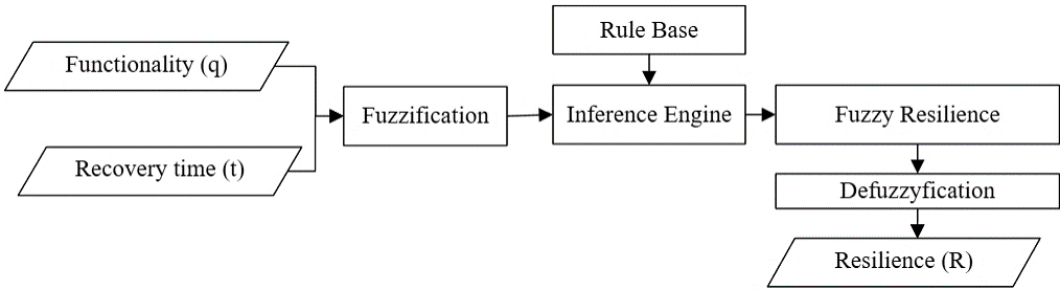

Figure 4. The Algorithm to calculate the resilience of a physical infrastructure indicator

2.1. Functionality Calculation Using Fragility Analysis

A fragility analysis is a probabilistic approach used to assess the likelihood of damage to a system, building, or component when exposed to an external hazard, such as an earthquake, flood, or hurricane. It aims to assess the *P* resulting from a hazard intensity, providing input for a loss estimation, structural performance evaluation, disaster-resistant system design, risk mitigation decision-making, and other related purposes.

The main components of a fragility analysis are the hazard, *ds*, and fragility curve. The hazard is a parameter that describes the strength of a disaster event, such as the spectral acceleration (*Sa*) for earthquakes or maximum wind speed for hurricanes. Damage states (*ds*) are defined as the level of damage that can occur to an asset or building. It is generally divided into 4–5 categories, namely, *ds*0 (undamaged), *ds*1 (slight damage), *ds*2 (moderate damage), *ds*3 (extensive damage), and *ds*4 (complete damage). Research to define the *Sa* for the relevant *ds* of non-engineered residential buildings was conducted by Kristiawan et al. [11]. The new *Sa* is expected to produce more accurate results in the calculation process and comply with HAZUS-MH MR5 [30].

A fragility curve illustrates the likelihood of a building experiencing damage at various hazard intensities. Typically, this curve has an S-shape (sigmoid curve) and is based on a log-normal distribution.

The fragility curve depicted in Figure 5 describes the probability of a building experiencing structural and non-structural damage, based on an average spectral response estimate. Equation 1 represents the mathematical approach for calculating *P*.

$$P(ds|S_a) = \emptyset\left[\frac{1}{\beta_{ds}} ln \frac{S_a}{\bar{S}_{a,ds}}\right] \quad (1)$$

where ϕ is the standard cumulative distribution function, β is the standard deviation (*SD*) for uncertainty, *Sa* is the acceleration spectra at a certain level, $\bar{S}_{a,ds}$ is the mean of the *Sa* when a building experiences damage, *ds* is the damage state, *P* is the probability of damage, and *ln* is the natural logarithm.

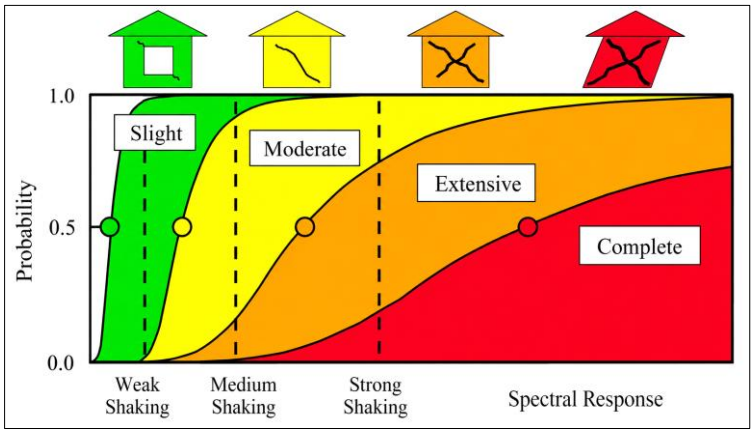

Figure 5. Fragility curve for slight, moderate, extensive, and complete damage [30]

Equation 2 is the total uncertainty of each *ds* (β_{ds}). The β_{ds} is a combination of uncertainty of the damage limit value, uncertainty in the structural capacity of the building under consideration, and uncertainty in the extent of the ground vibrations.

$$\beta_{ds} = \sqrt{[(CONV[\beta_c, \beta_d])]^2 + [\beta_{m(ds)}]^2} \quad (2)$$

where, β_c is the SD of the uncertainty in the structural capacity of the building; β_d is the SD of the uncertainty in the demand spectrum, with β_d=0.45 for short periods and β_d=0.5 for long periods; $\beta_{m(ds)}$ is the SD of the uncertainty in the damage limit value, which was set at 0.4; and CONV is the convolution. Equation 3 was used to calculate the β_c.

$$\beta_c = \sqrt{\ln(1 + \frac{s^2}{m^2})} \quad (3)$$

where, *m* is the average *Sa* capacity of the building, and *s* is the SD of the *Sa* capacity of the building.

A fragility curve was used to determine the *P*, which was calculated for each ds_1-ds_4. The *Sa* was set to range between 0.0–1.0g. The consequence function transformed the fragility curve into a vulnerability curve, which yielded the *E* (Equation 4).

$$\mathrm{E}(C|im) = \sum_{i=1}^{n} \mathrm{P}(ds_i|im) \times \mathrm{C}(ds_i) \quad (4)$$

where, $\mathrm{E}(C|i_m)$ is the expected consequence at a given intensity measure, $\mathrm{P}(\mathrm{ds}_i|\mathrm{im})$ is the probability of the i^{th} *ds*, and $\mathrm{C}(ds_i)$ is the i^{th} consequence

For Indonesia, there is currently no defined consequence function for *E*. Therefore, secondary data on consequences from various countries were used (Table 1). This approach of using consequence coefficients from multiple sources to achieve a more general result minimises potential bias, while the masonry characteristics of the residential buildings in those countries are quite similar to those in Indonesia. Future research is essential to determine the specific value of the consequence coefficients for *P* in Indonesia.

Table 1. Coefficient of consequences for buildings at each damage state level

Country	Damage State (DS)			
	Slight	Moderate	Extensive	Complete
Türkiye [31]	16%	33%	100%	100%
Australia [32]	10%	40%	75%	100%
Georgia [32]	10%	30%	80%	100%
Spain [33]	20%	40%	80%	100%
Italy [33]	10%	35%	75%	100%

Equation 5 is the estimated functionality value of a structure:

$$q = 1 - E(C|im) \quad (5)$$

where q is functionality and $\mathrm{E}(C|im)$ is the expected consequence at a given intensity measure.

2.2. Recovery Time

The recovery phase after the occurrence of a seismic disaster involves the initial recovery phase, which usually lasts between 1–3 months; the rehabilitation phase, which generally takes 3–12 months [34] ; and the reconstruction phase, which lasts for 1–5 years. The *t* after an earthquake is influenced by various factors, starting with the *ds*, the ability of the government and local government to provide a rehabilitation budget, and the social condition of the community [35]. The numerous factors involved in estimating the post-earthquake *t* provide an opportunity to use methods, such as multi-criteria approaches, to calculate a reasonable *t*. Finally, government authorities can determine the exact *t* as a reference for any recovery activities. The recovery time (*t*), which aligns with the *R*, indicates the optimal time for post-disaster recovery, which is reasonable for recovery activities.

This research proposed modeling t as a normalized value (0–1) that is flexible and can accommodate the exact *t*, recognizing that post-earthquake recovery duration is highly policy-dependent and context-specific rather than deterministic. The model considers a bounded recovery time range, representing the longest plausible duration under constrained resources and the shortest duration under favorable recovery conditions. For instance, the longest *t* required was five years (very long) to facilitate the process of calculating the *R*, resulting in a range of 0–0.1. This

indicated that the *t* for the long classification ranged from 2.5–4.5 years, and so on. Figure 6 shows the normalized *t* scale used in this research.

0 - 0.1	0.1	0.1 -0.5	0.5 - 0.9	0.9 - 1
Very Long	Long	Moderate	Short	Very Short

Figure 6. Normalized time scale of the recovery time of the model

2.3. Fuzzy Inference

Fuzzy logic (FL) is a concept that mimics human reasoning. It is the opposite of Boolean logic, which only has two possibilities, namely, YES or NO. The FL approach mimics human decision-making, where all the possibilities fall into two opposing values, namely, YES and NO. Like Boolean logic (0 and 1), FL allows values in between. Fuzzy logic (FL) does not provide accurate or exact reasoning but rather acceptable reasoning and helps handle uncertainty in engineering. Figure 7 illustrates the difference between Boolean logic and FL, where changes in FL values occur gradually.

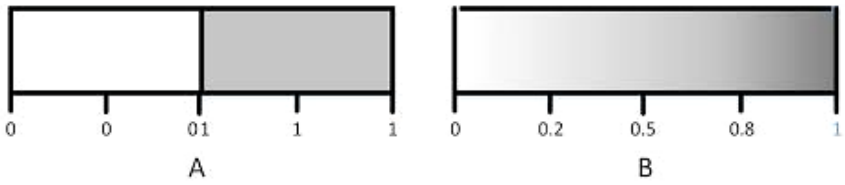

Figure 7. Boolean Logic (A) vs Fuzzy Logic (B)

An FL system comprises four main components, namely, a fuzzifier, a set of rules, an inference engine, and a de-fuzzifier. The process begins by gathering crisp input data and converting it into a fuzzy set through the use of fuzzy linguistic variables, fuzzy linguistic rules, and membership functions. This initial step is referred to as fuzzification. Next, inferences are drawn based on the established rules. Finally, the resulting fuzzy output is transformed back into crisp output using membership functions in the de-fuzzification step.

Well-known inference methods include the Tsukamoto Method [28, 36], Mamdani [37-39], and Takagi Sugeno [40-42]. The Tsukamoto inference has several advantages over Mamdani or Takagi-Sugeno methods, such as lower computational complexity and a unique crisp output value (consistency) [43].

The Tsukamoto fuzzy inference system is one of the methods used in FL systems to perform reasoning (inference) based on "IF-THEN" rules, with the characteristics of the consequences, the THEN part of each rule, being in the following form:

Rb: *If* x is A *and* y is B, *then* z is C (6)

where, *Rb* is the rule base, *x* and *y* are the input variables, *A* and *B* are the input sets, ***z*** is the output, and *C* is the output set. The degree of rule membership is calculated using fuzzy operators, usually the minimum for AND. For example, if the degree of membership of *x* to *A*=0.6, and *y* to *B*=0.8, then the degree of truth of the rule (α) is min(0.6, 0.8)=0.6. The final result was obtained using the weighted average formula:

$$z = \frac{\sum \alpha_i z_i}{\sum \alpha_i} \quad (7)$$

where α_i is the alpha predicate of the i^{th} rule, and $\boldsymbol{z_i}$ is the crisp output of the i^{th} rule.

3. Results and Discussion

3.1. Membership Function

In FL, a membership function maps each input value to a degree of membership in a fuzzy set, with values ranging from 0 to 1. Figures 8 to 10 show the membership functions of *q*, *t*, and *R* of the proposed model, which had been adapted and modified from Kammouh et al. [44]. The relationship between the variables in the membership function was arranged in a linear function in the Cartesian coordinate system. The crisp and fuzzy values were obtained by interpolating based on the coordinate points of intersection between the horizontal axis (crisp) and vertical axis (fuzzy) values. This was applied to the membership functions in Figures 8 to 10.

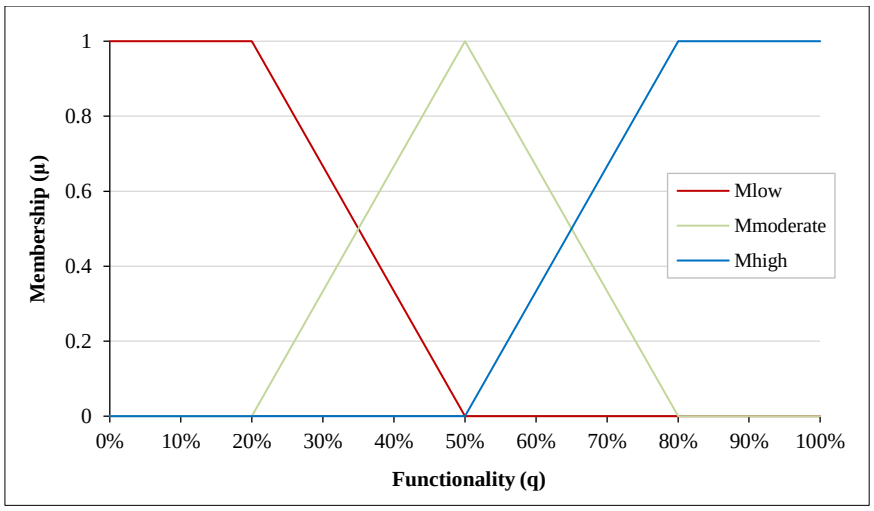

Figure 8. The membership function of functionality (q)

The membership functions for *q* were low, moderate, and high (Figure 8). Equations 8 to 10 were used to determine their fuzzy values. The input was the building's *q* (0–100%), and the result was a fuzzy value between 0–1. The next was a sample code written in Python [45, 46], explaining how to translate a membership function into a code. The Mlow(x) function represents the low membership function, where *f* is a variable for *q* in crisp. The Python codes for the other membership functions have been omitted for the sake of conciseness.

```
def Mlow(f):
    if f<=0.20:
        return 1.0
    elif 0.20<f<0.50:
        return (0.50-)/(0.50-0.20)
    else:  # f >= 0.50
        return 0.00
```

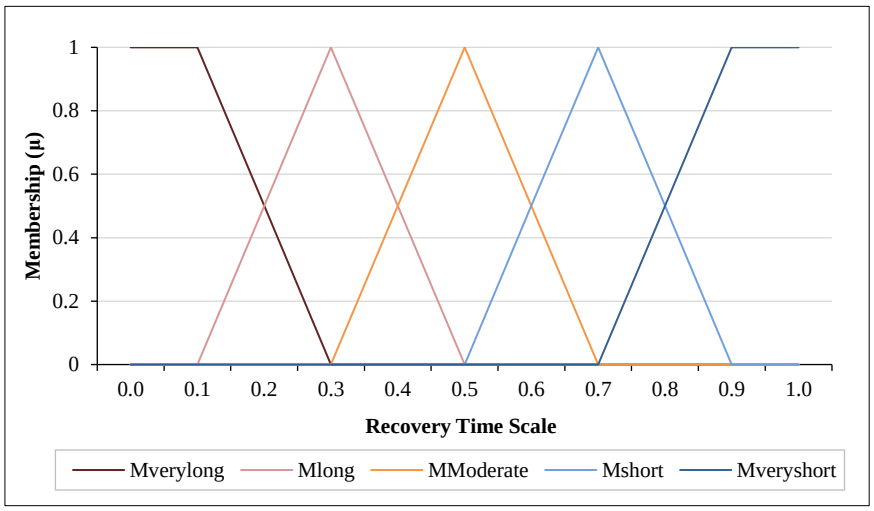

Figure 9. The membership function of recovery time

The membership functions for *t* were very short, short, moderate, long, and very long (Figure 9). The following is the Python code for the very short membership function, where Mveryshort() is the function name.

```
def Mveryshort(r):
    if r<=0.10:
        return 1.0
    elif r<=0.30:
        return (0.30-r)/(0.30-0.10)
    else:
          return 0.00
```

The membership functions for *R* were not resilient, poorly resilient, moderate, resilient, and highly resilient (Figure 10). This membership function was used to de-fuzzify a fuzzy *R* value.

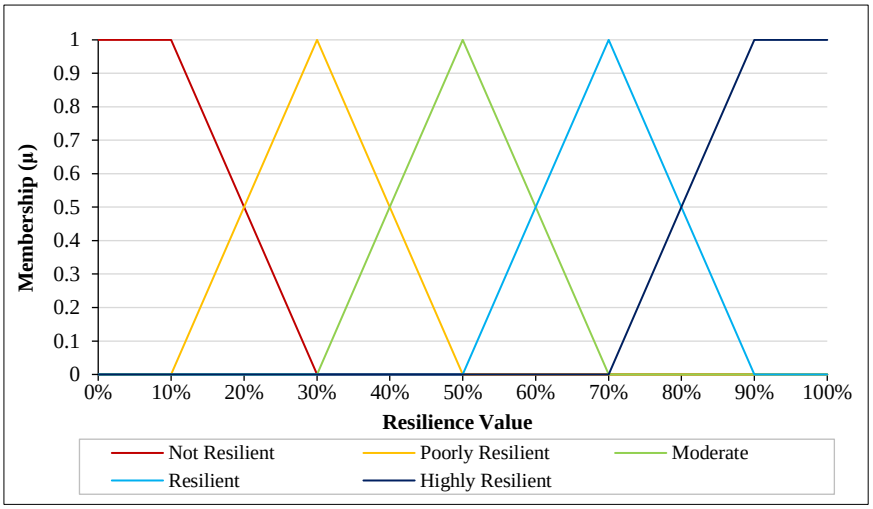

Figure 10. The membership function of resilience

The following is the Python code for the moderate membership function, which served as an inverse function. In the script, the *fr* variable was an input fuzzy value that was converted to a crisp value, yielding an *R*.

```
def Mmoderate (fr):
    if fr == 0:
        return 0.5
    elif 0 < fr <= 1:
        return 0.5 + fr * (0.7 - 0.5)
    else:
          raise ValueError ("FR must be in the range [0, 1]")
```

Based on expert judgment and commonly adopted resilience logic reported in previous studies, all the membership functions for *q*, *t*, and *R* were integrated to form the system's rule base (inference engine) (Table 2). As the rule base used the conjunction 'AND' to connect *q* and *t*, the algorithm used the minimum operator to determine the α for the predicate. All the α-predicates were combined with their corresponding *R* membership functions to yield a crisp *R*. Equation 7 was used to aggregate all the results from rules R1–R15 (*z*) to determine the final *R*.

Table 2. Fuzzy rule base for resilience calculation

Code	Rule
R1	If Functionality is High AND Recovery time is Very Short THEN Highly Resilient
R2	If Functionality High AND Recovery time is Short THEN Highly Resilient
R3	If Functionality High AND Recovery time is Moderate THEN Highly Resilient
R4	If Functionality High AND Recovery time is Long THEN Moderate
R5	If Functionality High AND Recovery time is Very Long THEN Moderate
R6	If Functionality Moderate AND Recovery time is Very Short THEN Resilience
R7	If Functionality Moderate AND Recovery time is Short THEN Resilient
R8	If Functionality Moderate AND Recovery time is Moderate THEN Moderate
R9	If Functionality Moderate AND Recovery time is Long THEN Poorly Resilience
R10	If Functionality Moderate AND Recovery time is Very Long THEN Poorly Resilient
R11	If Functionality Low AND Recovery time is Very Short THEN Moderate
R12	If Functionality Low AND Recovery time is Short THEN Moderate
R13	If Functionality Low AND Recovery time is Moderate THEN Not Resilient
R14	If Functionality Low AND Recovery time is Long THEN Not Resilient
R15	If Functionality Low AND Recovery time is Very Long THEN Not Resilient

Figure 11 illustrates the results of a sensitivity analysis for the calculation of *R* at the indicator level. Upon analysis, the constant values of *q* and *t* were defined as 0.5. The result indicated that *R* increased as *q* or *t* increased, although slight fluctuations occurred due to the overlapping of *q* or *t*.

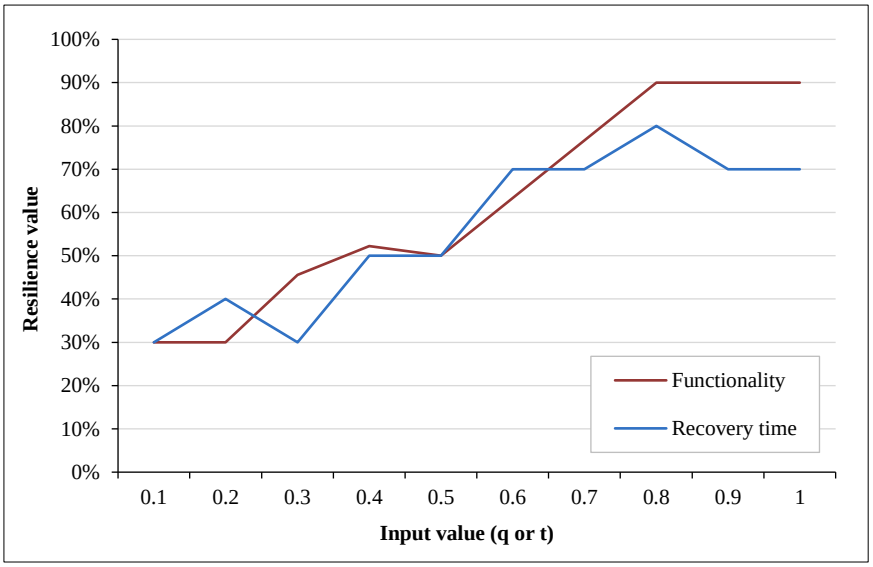

Figure 11. Sensitivity Analysis on variable q and t at the indicator resilience value

3.2. Residential Building Functionality Calculation

The following explains the calculation of the *q* of residential buildings as part of a building construction component based on an earthquake hazard scenario in Surakarta City. Several steps were required to evaluate the *q* of a residential building. First, a residential building survey was conducted to classify the attributes of the residential building. Next, a detailed survey of the residential building was carried out to collect geometrical data on the building, including its materials, such as concrete and reinforcing steel, as well as its location. The data were used to build a geometrical model of the building, including the loading, such as dead load, additional dead load, and live load, as well as seismic and lateral loads, in accordance with the standards issued by the Indonesian Government [47]. A fragility analysis was conducted to assess the vulnerability of the building and determine its remaining *q* after a seismic disaster.

The seismic loading design was calculated using the Spectra Response Design, which was adapted to the area where the building to be evaluated was located [48]. A random data collection survey was conducted on approximately 252 residential buildings in Surakarta City. Figure 12 shows several one- and two-story residential buildings that were recorded.

Figure 12. Residential buildings in Surakarta City

Table 3 lists the residential building types in Surakarta City from the survey, classified by the number of floors. Most of the residential buildings in Surakarta City were one-story buildings (66.27%), followed by two-story buildings (32.14%). Additionally, there were three- and five-story buildings, comprising approximately 1.59% of the total. In general, the residential buildings in Surakarta City were low-rise.

Table 3. Residential building data in Surakarta City is distributed based on the number of stories in each building

Stories	Amount	Percentage
1	167	66.27%
2	81	32.14%
3	3	1.19%
4	0	0.00%
5	1	0.40%
Total	**252**	**100.00%**

Figure 13 is the sample data model that was analyzed using Seismostruct. The sample data consisted of one- and two-story residential buildings, which formed the majority of the buildings in Surakarta City. The results showed the capacity curve, capacity spectrum, fragility curve, and vulnerability curve or *E*.

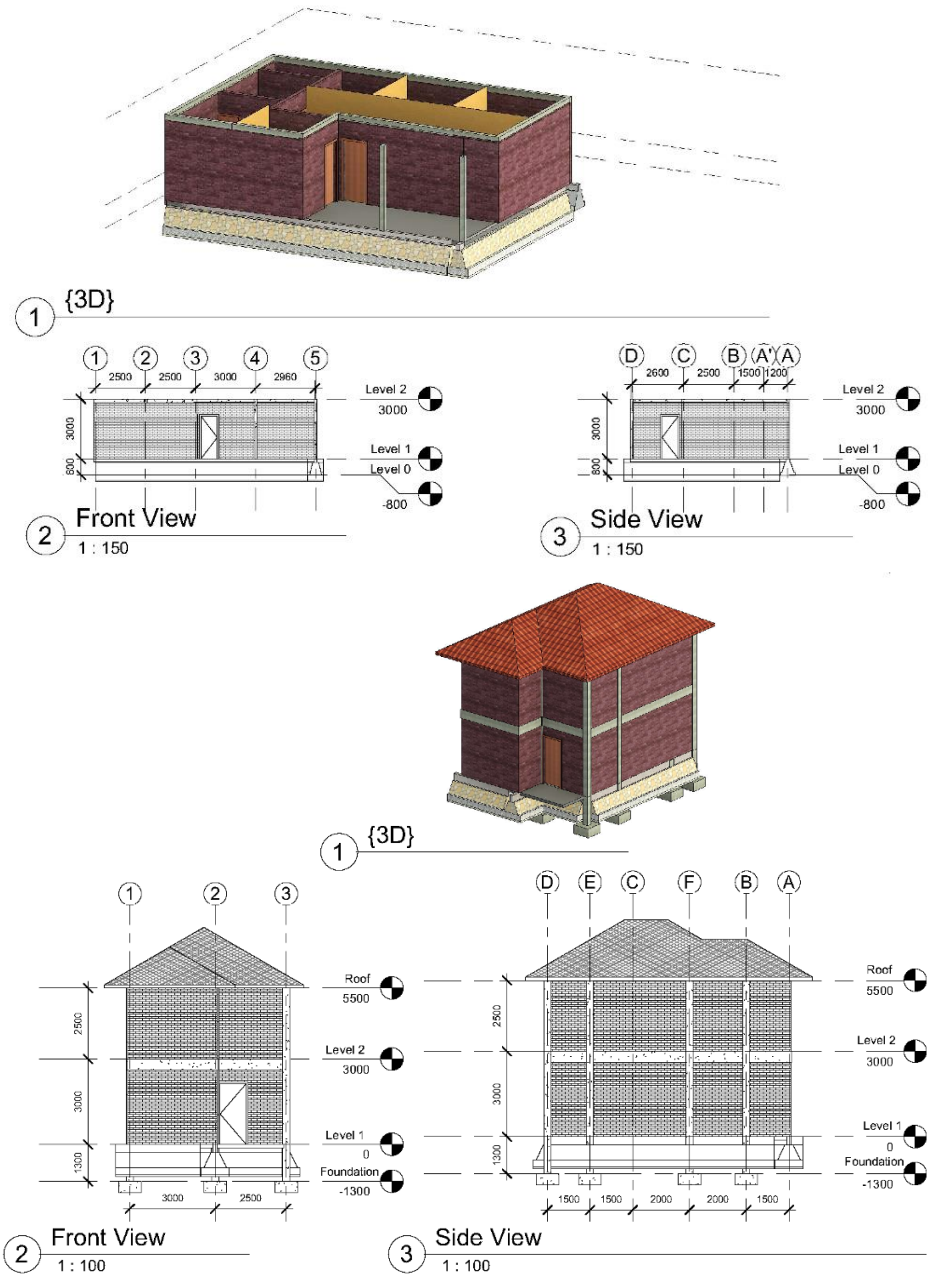

Figure 13. 3D models of one and two-story houses surveyed in Surakarta City

The Spectral Response Design was used to adjust the applied seismic loading design to the Surakarta City area [48]. Based on the coordinates of Surakarta City, the seismic parameters were *Fa*=1.1988, *Fv*=1.9900, site class of *SD*

(moderate), and *PGA*=0.3513. The response acceleration parameter in the short period (S_{DS}) was 0.6373, and the 1-second period (S_{D1}) was 0.5174. Based on the S_{DS} and S_{D1}, Surakarta City was included in the *D* risk category for earthquake-resistant buildings. The fragility of the one- and two-story residential buildings was calculated using the *ds* for non-engineered buildings, based on the findings of Kristiawan et al. [11]. The results of the fragility analysis conducted using Seismostruct for the one- and two-story buildings yielded the fragility curves shown in Figures 14 and 15, indicating that the one-story buildings were more fragile than the two-story buildings, possibly due to differences in building material quality.

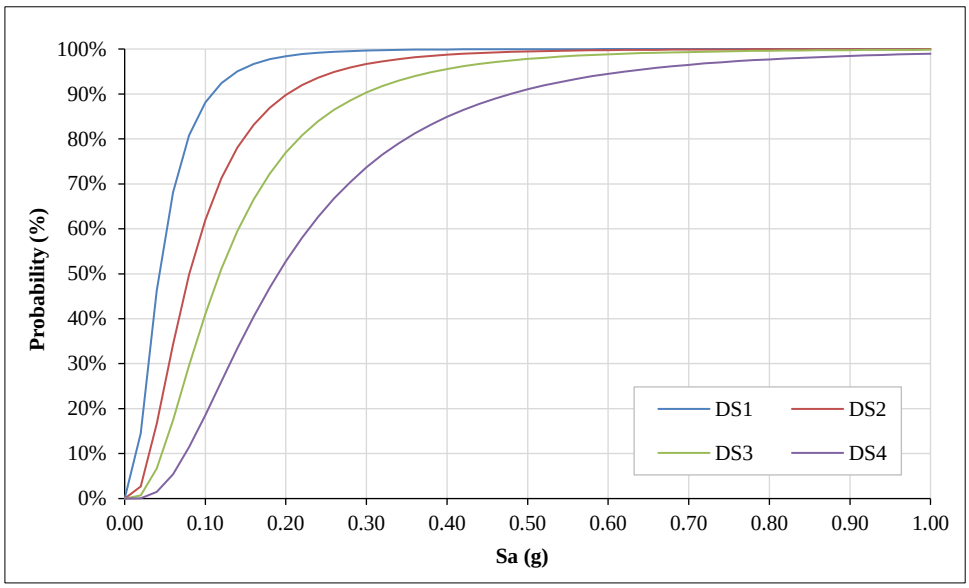

Figure 14. The fragility curve of one-story residential buildings in Surakarta City

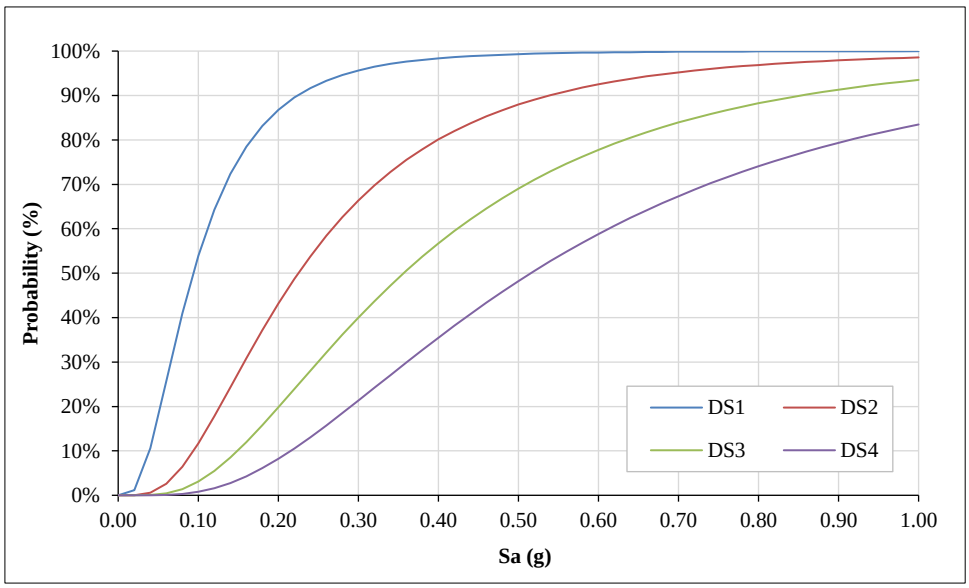

Figure 15. The fragility curve of two-story residential buildings in Surakarta City

The consequence function converted the fragility curve into a vulnerability curve, illustrating the *E* of the assessed buildings. According to Ali et al. [49], there are three categories of *ds* for buildings, namely, light damage (≤35%), moderate damage (35–45%), and heavy damage (≥45%).

The Seismostruct results showed that the one-story residential buildings had a maximum base shear of 25.26 kN at a displacement of 0.06 m, while the two-story residential buildings had a base shear of 414.93 kN at a displacement of 0.12 m at *Sa*=0.2 g, so that the scenario of *Sa* used a range of between 0.06–0.20 g (Table 4). Equation 4 was used to calculate the *E* and produce the vulnerability curve. The results are presented in Tables 4 and 5, and Figures 16 and 17. The graphs in Figures 16 and 17 indicate that the *E* of the one-story residential buildings was higher than that of the two-story buildings.

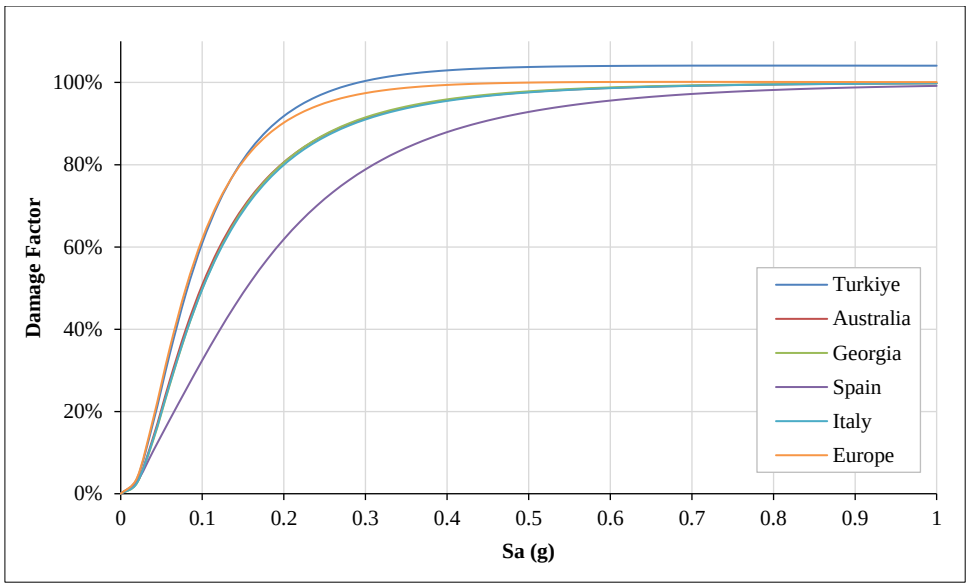

Figure 16. Vulnerability curves for one-story residential buildings

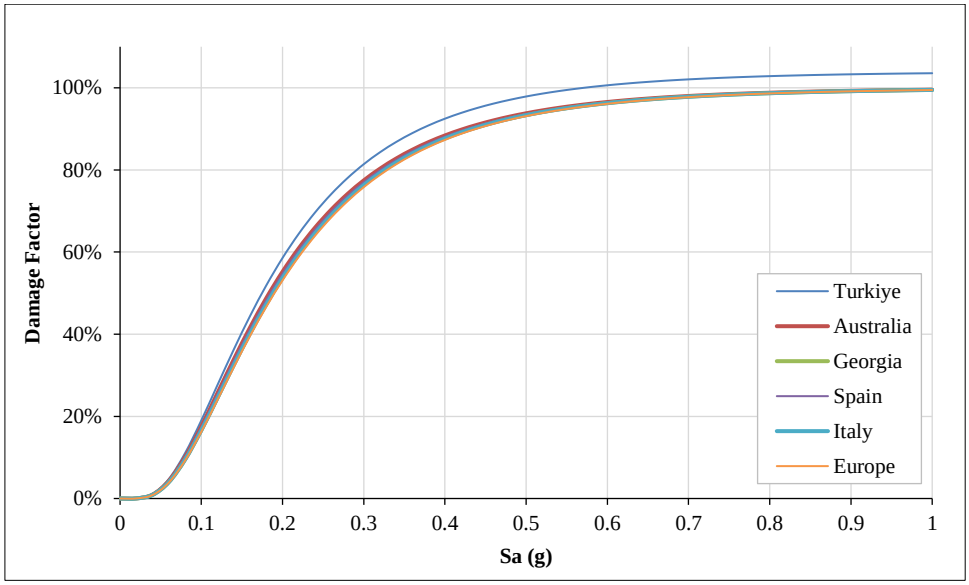

Figure 17. Vulnerability curves for two-story residential buildings

Tables 4 and 5 provide the *E*, with the referenced *Sa*=0.16 g, of the one- and two-story buildings, respectively. The *P* of the one-story residential buildings was greater than that of the two-story residential buildings, indicating that the latter were stronger and of a higher quality.

Table 4. The expected consequence (damage) of a one-story residential building at various Sa values.

Coefficient of Consequences	Percentage of Damage			
	Sa=0.06g	Sa=0.12g	Sa=0.16g	Sa=0.2g
Türkiye	9.65%	36.70%	52,68%	65,14%
Australia	8.46%	33.42%	48,61%	60,67%
Georgia	8.32%	33.08%	48,25%	60,33%
Spain	7.83%	31.08%	45,69%	57,60%
Italy	8.36%	33.16%	48,32%	60,39%
Europe	9.60%	36.11%	51,56%	63,52%
Average	8.70%	36.70%	49,18%	61,27%

Table 5. The expected consequence (damage) of a two-story residential building at various Sa values.

Consequences coefficient	Percentage of Damage			
	Sa = 0.06g	Sa = 0.12g	Sa = 0.16g	Sa = 0.2g
Türkiye	0.17%	2.66%	6.48%	11.69%
Australia	0.15%	2.41%	5.95%	10.81%
Georgia	0.14%	2.34%	5.80%	10.58%
Spain	0.18%	2.71%	6.51%	11.65%
Italy	0.14%	2.37%	5.86%	10.67%
Europe	0.17%	2.70%	6.53%	11.72%
Average	0.15%	2.53%	6.19%	11.18%

According to Table 3, the distribution of residential buildings indicates that single-story structures account for 66.27% of the total, while two-story buildings comprise 32.14%. For the sake of analysis, these proportions are rounded to 67% and 33%, respectively. By using Equation 5 and the data from Tables 4 and 5, we can calculate the average functionality of these buildings using the center-of-area method (Table 6).

Table 6. The functionality value of residential buildings at various Sa values

Building Type	Functionality			
	Sa=0.06g	Sa=0.12g	Sa=0.16g	Sa=0.2g
1-story residential building	91.30%	63.30%	27.57%	19.16%
2-story residential buildings	95.15%	84.09%	75.49%	67.02%
Average	92.57%	70.16%	43.38%	34.95%

3.3. Resilience Calculation of Residential Buildings in Surakarta

The following example is a simulation of an earthquake striking Surakarta City, with the referenced *Sa*=0.16 g. The *q* of the residential buildings was set at 43.38%. This scenario illustrates how alternative recovery-time assumptions can be evaluated to assess the resulting resilience level of the residential building sector.

Table 7 outlines the process of calculating the *R* of the residential buildings, alongside the fuzzy rule base detailed in Table 2, to address the question. The *R* for the residential buildings in the applied scenario was set at 52.47%. As seen in Figure 10, the residential buildings were moderately resilient.

Table 7. Calculation of the alpha predicate and z values

No.	Functionality(Q)		Recovery time (T)		Alpha Predicate	Z		Alpha * Z
1	High	0.0000	Very Short	0	0.0000	Highly Resilient	70.0%	0.00%
2	High	0.0000	Short	0	0.0000	Highly Resilient	70.0%	0.00%
3	High	0.0000	Moderate	1	0.0000	Highly Resilient	70.0%	0.00%
4	High	0.0000	Long	0	0.0000	Moderate	70.0%	0.00%
5	High	0.0000	Very Long	0	0.0000	Moderate	70.0%	0.00%
6	Moderate	0.7793	Very Short	0	0.0000	Resilient	90.0%	0.00%
7	Moderate	0.7793	Short	0	0.0000	Resilient	90.0%	0.00%
8	Moderate	0.7793	Moderate	1	0.7793	Moderate	54.4%	42.41%
9	Moderate	0.7793	Long	0	0.0000	Poorly Resilient	50.0%	0.00%
10	Moderate	0.7793	Very Long	0	0.0000	Poorly Resilient	50.0%	0.00%
11	Low	0.2207	Very Short	0	0.0000	Moderate	70.0%	0.00%
12	Low	0.2207	Short	0	0.0000	Moderate	70.0%	0.00%
13	Low	0.2207	Moderate	1	0.2207	Poorly Resilient	45.6%	10.06%
14	Low	0.2207	Long	0	0.0000	Not Resilient	30.0%	0.00%
15	Low	0.2207	Very Long	0	0.0000	Not Resilient	30.0%	0.00%
Resilience Value								**52.47%**

3.4. Discussion

The proposed methodology combines a fragility analysis with a fuzzy-logic model using the Tsukamoto inference. This contrasts with Tasmen et al. [17], who used dynamic Bayesian networks, and Wang et al. [20], who considered *R*-based recovery curves. Both the Bayesian and system-based models assume probabilistic state transitions. This approach converts *P* into linguistic rules and is a convenient compromise between inferring and maintaining uncertainty. Compared to Jia et al. [25], this model, which uses life cycle and multi-indicator aggregation, remains small and feasible.

Most of the studies surveyed here addressed uncertainty using probabilistic methods. The same can be said of the fragility-based literature [18, 21], time-variant deterioration modeling [22], and what concerns the Bayesian inference in [17]. This research framework addresses uncertainty by fuzzy sets and rule-based reasoning and directly relates to *E*, *q*, and *t* without the need for big datasets. This method does not depend on post-event observations, unlike empirical estimates for fragility, and is an ideal solution, especially in regions with limited data [18].

Several papers considered damage and recovery in temporal sequence. Fragility analyses [17, 20] cease at *P*. Recovery-oriented works [18, 19] model recovery as a restoring function since it often presumes fixed recovery functions. This research model directly binds the *q* and normalized *t* into a single inference system. This way of coupling is more akin to the decision logic used in practice. It contrasts with Chen et al. [22], where recovery enters the picture and interacts with degradation over time, but is still completely numerical and parameter-driven.

The result focuses on the monotonic and crisp recovery indices based on the Tsukamoto inference. This is an advantage over probabilistic outputs, which need to be further interpreted. The identified studies did not explicitly highlight monotonicity in terms of inference characteristics. The *R*-level output supports policy thresholds and prioritization, in line with the planning-related objectives of Tasmen et al. [17] and Wang et al. [20], with less computational cost.

The scenario-based simulation with Sa = 0.16 g resulted in a transparent and interpretable conclusion for Surakarta City. The hypothesis was also tested and confirmed by several empirical works, including Altunışık et al. [18], which concentrated on the perceived *ds* and not on the *R* categorization. Regional models [20] work at broader scales and do not produce city-level sharp indices. A moderate *R* suggested a moderate functional loss and recovery rate. This conclusion was also compatible with the functional recovery results presented in Altunışık et al. [18] and Wang et al. [20].

Generally, the presented works focused on probabilistic, empirical, or life-cycle R modeling. This paper proposed a rule-based, interpretable model that combined fragility, *q*, and *t* in a single step. The primary novelty is in the simplicity, transparency, and direct policy applicability, particularly in urban systems with scarce post-earthquake data.

4. Conclusion

A probabilistic *R* evaluation model for residential buildings was developed in this study by integrating a fragility analysis and a fuzzy-logic approach with the Tsukamoto inference. The proposed model aimed to unify the uncertainty relationship between the *q* and *t* of residential buildings after a seismic disaster. The *q* was calculated using a fragility analysis, with *t* being expressed as a normalized value. The seismic intensity was the input to the fragility analysis to obtain the *P* and, subsequently, the *q* of the system. The *q* and normalized *t* were processed in a fuzzy logic environment using the Tsukamoto inference system to compute the *R* index. The use of the Tsukamoto inference system ensured monotonic, crisp outputs, making the resulting *R* useful for a decision-making policy by the authorities in disaster risk management and urban *R* planning. The flexibility of the model allows it to be applied to diverse seismic scenarios and urban contexts.

The simulation of the developed model was implemented for a case of one- and two-story residential buildings as part of the urban physical infrastructure. The simulation of the applied scenario, at Sa = 0.16 g, resulted in an average resilient *q* of 43.38%. The obtained *q*, combined with a medium *t* (0.5), yielded a residential building *R* of 52.47% in Surakarta City, which was classified as moderately resilient. This indicates that at Sa = 0.16 g, residential buildings in Surakarta City experience moderate functional loss and can recover within a moderate timeframe. The model can help authorities as a decision-support tool to mitigate seismic disasters.

5. Declarations

5.1. Author Contributions

Conceptualization, S.S., S.A.K., and N.M.; methodology, S.S.; software, S.; validation, S.S., S.A.K., N.M., and S.; data curation, S.S.; writing—original draft preparation, S.S., S.A.K., and S.; writing—original draft preparation, S., S.S., S.A.K., and N.M.; writing—review and editing, S.; visualization, S.S.; supervision, S.S., S.A.K., and N.M.; project administration, S.; funding acquisition, S. All authors have read and agreed to the published version of the manuscript.

5.2. Data Availability Statement

The data presented in this study are available on request from the corresponding author.

5.3. Funding and Acknowledgments

The authors would like to acknowledge the support provided by Sebelas Maret University through the Doctoral Dissertation Research Grant (Contract No. 228/UN27.22/PT.01.03/2023) for funding this research. All thanks are also given to all colleagues who have provided support during data collection.

5.4. Conflicts of Interest

The authors declare no conflict of interest.

6. References

[1] Prestianta, A. M., Fakhruddin, I., & Kustiwa, A. (2023). Communication Independence of Panggarangan Village Residents in the Scope of Disasters. Jurnal Sinergitas PKM & CSR, 7(1), 1–13. doi:10.19166/jspc.v7i1.6150. (In Indonesian).

[2] Pribadi, K. S., Abduh, M., Wirahadikusumah, R. D., Hanifa, N. R., Irsyam, M., Kusumaningrum, P., & Puri, E. (2021). Learning from past earthquake disasters: The need for knowledge management system to enhance infrastructure resilience in Indonesia. International Journal of Disaster Risk Reduction, 64. doi:10.1016/j.ijdrr.2021.102424.

[3] Tenerelli, P., Gallego, J. F., & Ehrlich, D. (2015). Population density modelling in support of disaster risk assessment. International Journal of Disaster Risk Reduction, 13, 334–341. doi:10.1016/j.ijdrr.2015.07.015.

[4] Henrich, L., McClure, J., & Crozier, M. (2015). Effects of risk framing on earthquake risk perception: Life-time frequencies enhance recognition of the risk. International Journal of Disaster Risk Reduction, 13, 145–150. doi:10.1016/j.ijdrr.2015.05.003.

[5] Griffin, C., Ellis, D., Beavis, S., & Zoleta-Nantes, D. (2013). Coastal resources, livelihoods and the 2004 Indian Ocean tsunami in Aceh, Indonesia. Ocean and Coastal Management, 71, 176–186. doi:10.1016/j.ocecoaman.2012.10.017.

[6] Pramumijoyo, S. (2009). Road to earthquake mitigation: Lesson learnt from the Yogyakarta earthquake 2006. Journal of Applied Geology, 1(2), 32-36. doi:10.22146/jag.6672.

[7] Pradono, M. H. (2018). Building Vulnerability Assessment Following the Lombok Earthquake of August 5, 2018. Jurnal Alami : Jurnal Teknologi Reduksi Risiko Bencana, 2(2), 82. doi:10.29122/alami.v2i2.3109.

[8] Sihombing, Y. I., Adityawan, M. B., Chrysanti, A., Widyaningtias, W., Farid, M., Nugroho, J., Kuntoro, A. A., & Kusuma, M. A. (2020). Tsunami Overland Flow Characteristic and Its Effect on Palu Bay Due to the Palu Tsunami 2018. Journal of Earthquake and Tsunami, 14(2). doi:10.1142/S1793431120500098.

[9] Sugiarto, B., & Tohari, A. (2023). Unraveling the Enigma of the 2022 Cianjur Earthquake: Insights from Gravity Satellite Data. 2023 IEEE Asia-Pacific Conference on Geoscience, Electronics and Remote Sensing Technology (AGERS), 203–206. doi:10.1109/AGERS61027.2023.10490867.

[10] Bradley, K., & Hubbard, J. (2024). Magnitude 6.4 earthquake rocks Java, Indonesia: An unusual shallow earthquake near Bawean Island was felt widely across Indonesia and surrounding areas. Earthquake Insights. Available online: https://earthquakeinsights.substack.com/p/magnitude-64-earthquake-rocks-java (accessed on April 2026).

[11] Kristiawan, S. A., Safarizki, H. A., Purwanto, E., Sangadji, S., Trisnawan, A. D., & Nugroho, T. S. (2024). Damage State of Non-Engineered Residential Buildings Owing To Earthquakes: a Case Study in Pacitan Regency, Indonesia. Civil and Environmental Engineering, 20(1), 426–439. doi:10.2478/cee-2024-0033.

[12] Cimellaro, G. P. (2016). Resilience indicators. Geotechnical, Geological and Earthquake Engineering, 41, 49–69. doi:10.1007/978-3-319-30656-8_3.

[13] Kammouh, O., & Cimellaro, G. P. (2018). PEOPLES: A Tool to Measure Community Resilience. Structures Conference 2018, 161–171. doi:10.1061/9780784481349.015.

[14] Renschler, C. S., Frazier, A. E., Arendt, L. A., Cimellaro, G. P., Reinhorn, A. M., & Bruneau, M. (2010, July). Developing the 'PEOPLES'resilience framework for defining and measuring disaster resilience at the community scale. Proceedings of the 9th US national and 10th Canadian conference on earthquake engineering, 25-29 July, 2010, Canada Toronto.

[15] Cimellaro, G. P., Renschler, C., Reinhorn, A. M., & Arendt, L. (2016). PEOPLES: A Framework for Evaluating Resilience. Journal of Structural Engineering, 142(10), 04016063. doi:10.1061/(asce)st.1943-541x.0001514.

[16] Chrysafiadi, K. (2023). Fuzzy Logic. - Fuzzy Logic-Based Software Systems. Learning and Analytics in Intelligent Systems, Volume 34, Springer, Cham, Switzerland. doi:10.1007/978-3-031-44457-9_1.

[17] Tasmen, T., Sen, M. K., Hossain, N. U. I., & Kabir, G. (2023). Modelling and assessing seismic resilience of critical housing infrastructure system by using dynamic Bayesian approach. Journal of Cleaner Production, 428, 139349. doi:10.1016/j.jclepro.2023.139349.

[18] Altunışık, A. C., Sisman, R., Günaydin, M., Okur, F. Y., Yilmaz, Z., Sunca, F., Hadinata, P., Aslan, B., Sezdirmez, T., & Taciroglu, E. (2025). Empirical fragility curves for RC residential buildings after 2023 Kahramanmaraş, Türkiye earthquakes. Journal of Building Engineering, 111. doi:10.1016/j.jobe.2025.113446.

[19] Zhao, H., & Takahashi, N. (2025). Resilience Evaluation of Post-Earthquake Functional Recovery for Precast Prestressed Concrete Buildings. Applied Sciences (Switzerland), 15(13), 6994. doi:10.3390/app15136994.

[20] Wang, N., Sun, B., Chen, H., Chen, X., & Wang, H. (2024). The seismic resilience-based methodology of regional building function recovery assessment. Soil Dynamics and Earthquake Engineering, 180. doi:10.1016/j.soildyn.2024.108601.

[21] Naiel, A., Hanna, N., & Lotfy, I. (2025). Assessing seismic performance of mid-rise reinforced concrete buildings using fragility curves. Innovative Infrastructure Solutions, 10(1), 9. doi:10.1007/s41062-024-01750-9.

[22] Chen, Z., Feng, D. C., Cao, X. Y., & Wu, G. (2024). Time-variant seismic resilience of reinforced concrete buildings subjected to spatiotemporal random deterioration. Engineering Structures, 305. doi:10.1016/j.engstruct.2024.117759.

[23] Formisano, A., & Longobardi, G. (2025). Seismic fragility and energy efficiency upgrading of masonry compounds using lightweight aluminium alloy exoskeletons: a case study in South Italy. Bulletin of Earthquake Engineering, 1-19. doi:10.1007/s10518-025-02149-2.

[24] Dahal, L., Burton, H., & Zhong, K. (2025). High-Fidelity High-Resolution Regional Seismic Risk and Resilience Assessment of Large Building Inventories. Earthquake Engineering and Structural Dynamics, 54(5), 1376–1396. doi:10.1002/eqe.4313.

[25] Jia, S., Zhan, D. J., Jiang, H., & Ye, S. D. (2025). Life-cycle seismic resilience and sustainability assessment method of reinforced concrete buildings. Structures, 80, 109919. doi:10.1016/j.istruc.2025.109919.

[26] Gautham, A., & Gopi Krishna, K. (2017). Fragility Analysis - A Tool to Assess Seismic Performance of Structural Systems. Materials Today: Proceedings, 4(9), 10565–10569. doi:10.1016/j.matpr.2017.06.421.

[27] Frans, R. (2021). Seismic Fragility Analysis of Reinforced Concrete Structures. JUTEKS : Jurnal Teknik Sipil, 6(1), 17. doi:10.32511/juteks.v6i1.719.

[28] Sunardi, Yudhana, A., & Furizal. (2023). Tsukamoto Fuzzy Inference System on Internet of Things-Based for Room Temperature and Humidity Control. IEEE Access, 11, 6209–6227. doi:10.1109/ACCESS.2023.3236183.

[29] Kammouh, O., Zamani Noori, A., Domaneschi, M., & Cimellaro, G. P. (2018). Fuzzy Based Tool to Measure the Resilience of Communities. Maintenance, Safety, Risk, Management and Life-Cycle Performance of Bridges, 1895–1901, CRC Press, Boca Raton, United States. doi:10.1201/9781315189390-258. doi:10.1201/9781315189390-258.

[30] Sharma, A. K., & Setia, S. (2025). Analysis of irregular RC buildings using probabilistic seismic vulnerability assessment. Asian Journal of Civil Engineering, 26(9), 3785–3796. doi:10.1007/s42107-025-01397-6.

[31] Bal, I. E., Bommer, J. J., Stafford, P. J., Crowley, H., & Pinho, R. (2010). The influence of geographical resolution of urban exposure data in an earthquake loss model for Istanbul. Earthquake Spectra, 26(3), 619–634. doi:10.1193/1.3459127.

[32] D'Ayala, D., Meslem, A., Vamvatsikos, D., Porter, K., Rossetto, T., Crowley, H., & Silva, V. (2014). Guidelines for analytical vulnerability assessment of low/mid-rise buildings. GEM Technical Report, GEM Foundation, Pavia, Italy.

[33] Guardiola-Víllora, A., Molina, S., & D'Ayala, D. (2023). Performance based probabilistic seismic risk assessment for urban heritage. An example in Pla del Remei Area (Valencia). Bulletin of Earthquake Engineering, 21(10), 4951–4991. doi:10.1007/s10518-023-01721-y.

[34] Jibiki, Y., Pelupessy, D., Sasaki, D., & Iuchi, K. (2020). Implementation of post disaster needs assessment in Indonesia: Literature review. Journal of Disaster Research, 15(7), 975–980. doi:10.20965/jdr.2020.p0975.

[35] Suprayoga Hadi. (2019). Learning from The Legacy of Post-Disaster Recovery in Indonesia for The Acceleration of Post-Disaster Recovery in Lombok. Jurnal Perencanaan Pembangunan: The Indonesian Journal of Development Planning, 3(1), 14–31. doi:10.36574/jpp.v3i1.56.

[36] Olmedo-García, L. F., García-Martínez, J. R., Rodríguez-Reséndiz, J., Dublan-Barragán, B. S., Cruz-Miguel, E. E., & Barra-Vázquez, O. A. (2025). Tsukamoto Fuzzy Logic Controller for Motion Control Applications: Assessment of Energy Performance. Technologies, 13(9), 387. doi:10.3390/technologies13090387.

[37] Selvachandran, G., Quek, S. G., Lan, L. T. H., Son, L. H., Giang, N. L., Ding, W., Abdel-Basset, M., & De Albuquerque, V. H. C. (2021). A New Design of Mamdani Complex Fuzzy Inference System for Multiattribute Decision Making Problems. IEEE Transactions on Fuzzy Systems, 29(4), 716–730. doi:10.1109/TFUZZ.2019.2961350.

[38] Agustian, I., Prayoga, B. I., Santosa, H., Daratha, N., & Faurina, R. (2022). NFT Hydroponic Control Using Mamdani Fuzzy Inference System. Journal of Robotics and Control (JRC), 3(3), 374–383. doi:10.18196/jrc.v3i3.14714.

[39] Iqbal, K., Khan, M. A., Abbas, S., Hasan, Z., & Fatima, A. (2018). Intelligent transportation system (ITS) for smart-cities using Mamdani Fuzzy Inference System. International Journal of Advanced Computer Science and Applications, 9(2), 94–105. doi:10.14569/IJACSA.2018.090215.

[40] Samavat, T., Nazari, M., Ghalehnoie, M., Nasab, M. A., Zand, M., Sanjeevikumar, P., & Khan, B. (2023). A Comparative Analysis of the Mamdani and Sugeno Fuzzy Inference Systems for MPPT of an Islanded PV System. International Journal of Energy Research, 7676113. doi:10.1155/2023/7676113.

[41] Cavallaro, F. (2015). A Takagi-Sugeno fuzzy inference system for developing a sustainability index of biomass. Sustainability (Switzerland), 7(9), 12359–12371. doi:10.3390/su70912359.

[42] Rout, S. S., Misra, B. B., & Samanta, S. (2018). Competency mapping with Sugeno fuzzy inference system for variable pay determination: A case study. Ain Shams Engineering Journal, 9(4), 2215–2226. doi:10.1016/j.asej.2017.03.007.

[43] Ross, T. J. (2005). Fuzzy logic with engineering applications. John Wiley & Sons, Hoboken, United States. doi:10.1002/9781119994374.

[44] Kammouh, O., Noori, A. Z., Taurino, V., Mahin, S. A., & Cimellaro, G. P. (2018). Deterministic and fuzzy-based methods to evaluate community resilience. Earthquake Engineering and Engineering Vibration, 17(2), 261–275. doi:10.1007/s11803-018-0440-2.

[45] Joyce, P. (2022). Python Programming. In: C and Python Applications. APress, Berkeley, United States. doi:10.1007/978-1-4842-7774-4_1.

[46] de Groot, C. (2020). Installing Python. Python Basics. APress, New York, United States. doi:10.1007/978-1-4842-5831-6_3.

[47] Khala, C. C. S., Basyaruddin, B., & Dharmawan, S. (2022). Comparative Study of Existing Building Structure Performance Against SNI 1726:2019 and 1727:2020. Teras Jurnal : Jurnal Teknik Sipil, 12(2), 507–514. doi:10.29103/tj.v12i2.721. (In Indonesian).

[48] Surya Permana, C. B. (2021). Design Response Spectra Based on Earthquake Hazard Maps and Specific Soil Properties at Indonesian Ports According to SNI 1726 2019. Jurnal Teknik Sipil, 17(1), 41–54. doi:10.28932/jts.v17i1.3423.

[49] Ali, A. M., Sangadji, F. A., & Kempa, M. (2024). Analysis of the Level of Damage to the Rusunawa Building at IAIN Ambon. Kokoh, 22(1), 1–14. doi:10.17509/k.v22i1.66208. (In Indonesian).